Scientific Bulletin of Politehnica University Timisoara
Transactions on HYDROTEHNICS

Volume 70(84), Issue 1, 2025

STUDY OF AN ACCIDENTAL FLOOD WAVE TRANSIT ON A RIVER SECTOR, IN THE AREA OF A ROAD BRIDGE

Alina-Ioana Popescu-Bușan[1] Gheorghe Lazăr[1] Albert Titus Constantin[1] Marie Alice Ghițescu[1] Şerban-Vlad Nicoară[1]

Abstract: The paper presents three discrete numerical simulations of the water flow transit in the Timiș and Sebeș rivers confluence area, specifically at the crossing concrete road bridge on Teiuşului Street in the Town of Caransebeş. The simulation deals with the situation of an accidental flood wave with the special configuration given by the hydrographer occurred from 6th to 8th of April 2000. Following the three simulations carried out on numerical models developed in different ways – a 1D model for which the bridge was modeled by 4 cross-sections that include the two abutments and the two quadruple piers (each pier containing two pillars with a circular section) supporting the beams on which the runway rests; a 2D model in which the crossing bridge was considered as a connecting structure type; a 2D model in which the supporting elements of the crossing bridge (piers, abutments) were introduced as special 3D elements – a comparative study of the obtained results, specifically regarding water levels and flow velocities in non-permanent regime, was carried out. Each numerical model covers the same sections cut out of the two watercourses, in their confluence area.

Keywords: river engineering, flow numerical simulation, high waters flow, flow section throttling, water velocity distribution

1. GENERAL CONSIDERATIONS

The *HEC-RAS Mapper* in the *HEC-RAS package vers.6.2* [7] provides an efficient set of tools for the development of hydraulic models of rivers, both in *1D* and *2D*. In this work, the available tools will be used for the development of a couple of discrete numerical river models in *HEC-RAS*, with known geometric and hydraulic elements, as well as the presentation of the results in the area of a road bridge. Editing capabilities have been introduced within the *RAS Mapper* interface (see also [6;9]), allowing field editing and geometric data development operations in order to obtain an improved *1D* or *2D* numerical model and then also to visualize the post-processed results directly within the *HEC-RAS package*.

The *RASter Calculator* facility in the *HEC-RAS v.6.2 package allows* mathematical and logical operations to be performed on gridded datasets in *RAS Mapper* through user-defined scripts. In fact, a syntax is created for an established layer that can then be evaluated in *RAS Mapper* using interactive query tools. It is used to evaluate *RAS Normal* results in a very similar way to a dynamic map, in that it can animate the associated layer. If the established layer is used to compare the results from two different *HEC-RAS* simulations, then it is quite convenient to use the animated toolbar to evaluate at different time steps. However, an established layer can also have a static component layer, such as the *Terrain* layer.

An established layer is added to the *RAS Mapper* by selecting a *RAS* results group or by selecting the *Map Layers* group and choosing the *Create a New Calculated Layer* menu item used in the analysis. By default, land layers will always be available to the user.

As about the presented hydraulic study of a liquid flow transit on the Timiș and Sebeș rivers confluence, three discrete numerical simulations are performed, with a detailed approach in the vicinity of the confluence area at the road crossing bridge towards Teiuşului Street in the municipality of Caransebeş. The simulation was performed by considering a special hydrological phenomenon, meaning the occurrence of an accidental flood wave of a configuration given by the hydrographer developed from 6th to 8th of April 2000.

From these numerical simulations, a comparative study is carried out for the area of the crossing road-bridge. So, the water levels and flow velocities in non-permanent flow mode are estimated on the three different models: one numerical model in *1D* as associated to the reference ground (*Terrain_actual*) and two *2D* numerical models. The *1D* model considers the concrete road-bridge, represented by two quadruple pile (of circular section) abutment piers and the two side abutments, as modeled by four cross-sections. The *2D* models consider for the crossing a connection structure and respectively the bridge modeled by special *3D* elements for all the abutments. Each of the three discrete models covers the same sections from the two river courses.

[1] Faculty of Civil Engineering, Department of Hydrotechnical Engineering, Splaiul Spiru Haret No. 1/A, 300022, Timişoara, e-mail: alina.popescu-busan@upt.ro

2. DESCRIPTION OF THE THREE DISCRETE NUMERICAL MODELS

2.1 M1 – the *1D* numerical model

The location of the road-bridge that crosses the Timiş River covers a former flood zone, and therefore the Dâlmei Street had to be protected from flooding in the case of high waters, by a concrete parapet rising at height of approx. 0.90 m (see lower area - *Photo.1*).

Upstream of the site, a few hundred meters away (*Figure 1*), the Timiş River receives as a right tributary, the Sebeş River, which, in addition to the natural flows, also collects the tributary discharge from the Ruieni Hydropower Plant, transmitted to the river through the Zerveşti accumulation. Thus, the water flows can have normal variations between *3* and *54.5* m^3/s.

Photo 1. View of the crossing road-bridge, towards the Timiş River right bank; flood protection concrete parapet in the immediate front view

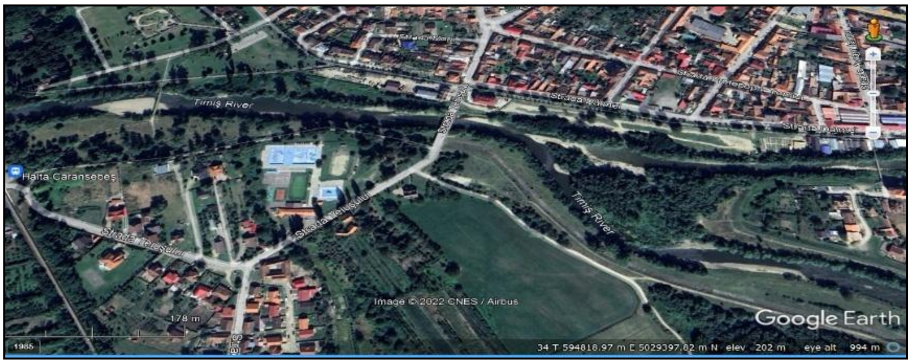

Figure 1. General view of the modeled site – Timiş - Sebeş Rivers confluence in Caransebeş

In a plan view, the route of the Timiş River towards the location of the bridge is not rectilinear and connects convexly to the bridge, and so, at high waters, the general flow is directed towards the right bank.

For modeling the geometry of the Timiş and Sebeş riverbeds, specifically of the confluence area, in the range of the municipality of Caransebeş, the following sections were considered: *Timiş River* – an upstream length from Caransebeş of 861 m, *Timiş River* – in Caransebeş for a length of 1162 m and *Sebeş River* – an upstream length from the confluence of 597 m. From these sections, a database was created by employing a situation plan (*Stereo 70*) and 19 cross profiles, these data highlighting the morphology of the minor and major riverbeds of the two rivers. Based on this consolidated database, a numerical model was created for the discrete model in *1D* (*Figure 2*), with the associated terrain: *Terrain_actual*. Its geometric extension is reduced with respect to the [10] and [11].

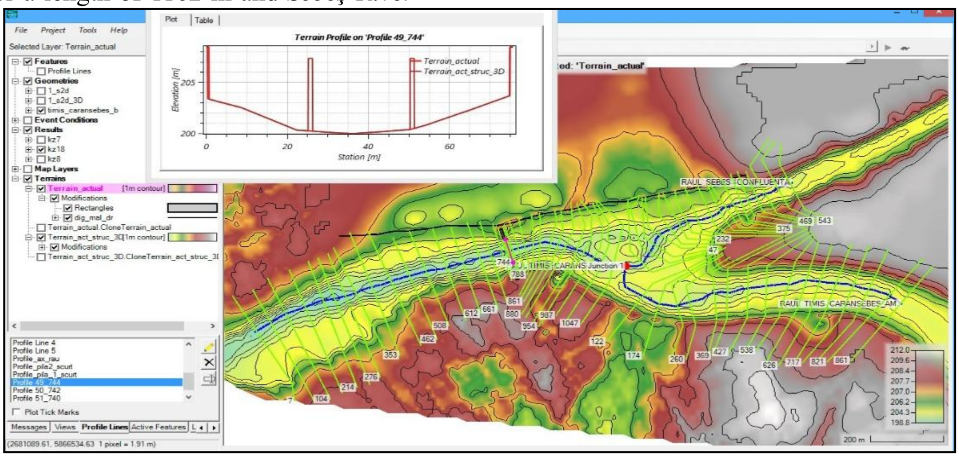

Figure 2. *1D* numerical model, situation plan view and cross-profile by the road bridge towards Teiuşului Street (location *739*) – *Terrain_actual* associated

From the overview (*Photo.1*) made from the right bank of the Timiș River (from Dâlmei Street), one can notice the two quadruple concrete abutment piers, each containing two columns of circular section supporting the beams on which the road track rests. On this discrete model (*Figure 2*) associated with the land (*Terrain_actual*), 4 cross-profiles are mainly significant as they define the two abutment piers and determine the geometry of the riverbed in the area related to the bridge in the minor and major riverbed.

2.2. M2– 2D NUMERICAL MODEL. CONNECTION STRUCTURE

In the *2D* developed model, the initial terrain model is employed and a *2D* surface domain, called *S2D*, is generated. It considers grid spacing of *Dx=10* and *Dy=10* (in meters) for which the associated model points and related cells hydraulic properties for are generated. In the *2D Flow Areas* directory, four perimeter domains are defined, comprising the areas of the two intermediate piers and the side abutments. An additional network tightening operation was performed by specifying the metric dimensions associated with the rectangular perimeters in *meters* (*Dx= 0.15, Dy=0.15*). The geometric dimensions of the regions associated with the two piers are *L=6.70m* and *B=1.30m*. The regions associated with the side abutments and embankments are *L=54.4m, B=6.70m* for the left bank and *L=33.52m, B=6.70m* for the right bank.

In the graphical representations in *Figure 3* and *Figure 4*, the *2D* analysis field and the connection structure introduced for establishing the geometry parameters, respectively, the hydraulic parameters necessary for discrete numerical modeling can be observed; all these elements are entered in the graphical window of the main menu of *HEC-RAS.*

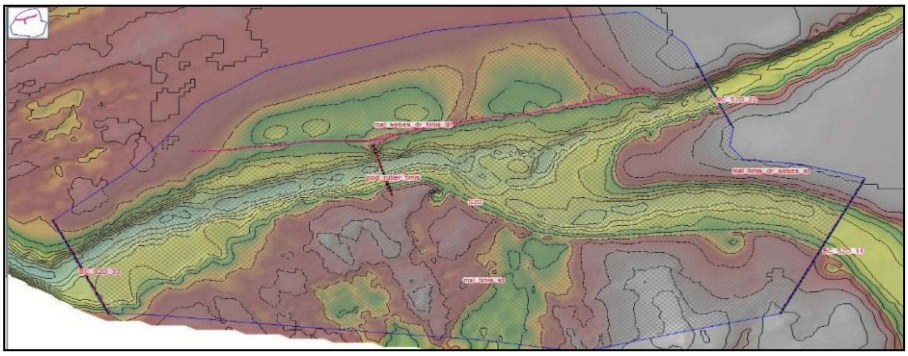

Figure 3. *2D* numerical model, connection structure at the road bridge

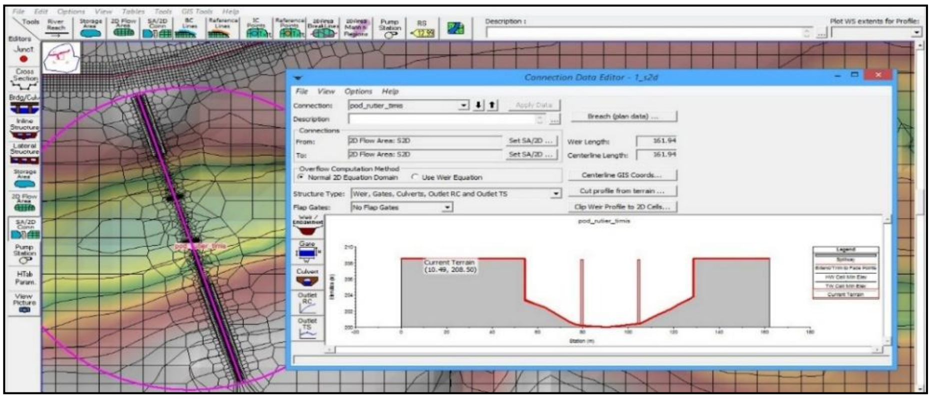

Figure 4. Geometry and hydraulic characteristics as associated with the connection structure at the road bridge

2.3. M3– 2D NUMERICAL MODEL. STRUCTURE WITH SPECIAL ELEMENTS *IN 3D*

Similarly, on the third discrete numerical model (*Figure 5*) associated with the land (*Terrain_act_struc_3D*), the two quadruple piers and, respectively, the left and right bank abutments are inserted in *3D*, as defining the geometry of the Timiș riverbed in the area of the road crossing bridge.

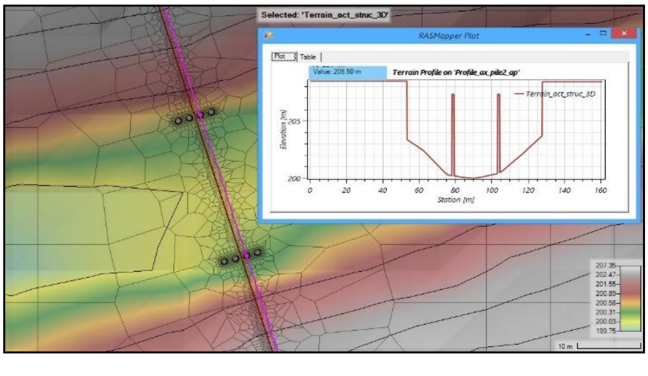

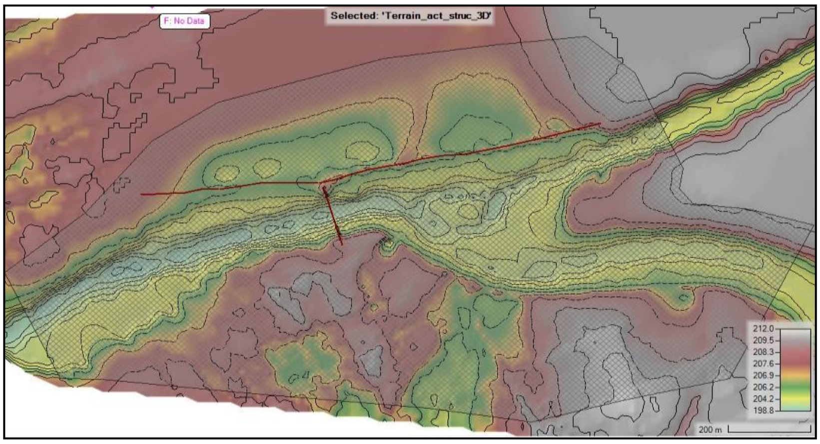

Figure 5. *2D* numerical model, *3D* special elements cross profile by the road bridge (side and intermediate abutments)

In the graphic representation of the discretization area in *Figure 6* (contour lines at an equidistance of *0.10m*) a longitudinal profile is also presented as intersecting the centers of the pillars at the two intermediate abutment piers in *alignments 1* and *2* on the left and right of the Timiș River, in location no.2.

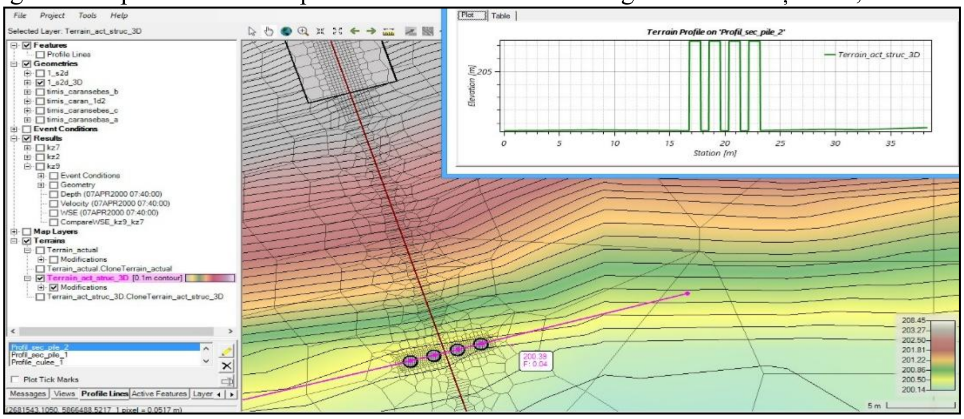

Figure 6. Meshing detail on the left intermediate quadruple abutment and longitudinal profile for alignment 2 (*3D* model)

3. BOUNDARY AND INITIAL CONDITIONS

Currently, the boundary conditions on the one-dimensional route [10/11] are the transit flows (by the shape of a known synthetic flood hydrograph) with a certain exceeding probability, attached to the upstream sections ("*543*" – on the Sebeş River and "*861*" – on the Timiş River), and respectively, the hydrodynamic slope as attached to the final section of the numerical model (section denoted with "*7*" – on the Timiş River).

For the initial conditions on the *M1* model, the start flow values are considered at the inlet sections as *15.5* m^3/s for each the Sebeş River in "*543*" and the Timiş River in "*861*", the sum of the downstream flow at the confluence (at "*1047*" section) being *31.00* m^3/s.

The configuration of the flood hydrograph on the Timiş River was established with a maximum value of *784,818* m^3/s, and for the hydrograph on the Sebeş River with the maximum value of *54.50* m^3/s. Currently, the margin conditions on the two-dimensional (*2D*) route, in terms of numerical values, are identical to those presented for the *M1 model*, except for the initial conditions where the water surface on the cells in the domain was initially considered. The starting level for the *2D* model is *204.30 mSL*.

For the *M2* and *M3* models, it was necessary to define the three *Boundary Conditions Lines* (BC Line) by the *BC Lines* option (see the names specified in *Figure 3*). In the case of this domain, two routes were defined in the upstream edges – *BC_S2D_11* on the Timiş River and *BC_S2D_22* on the Sebeş River, and respectively the route *BC_S2D_33* at the downstream edge on the Timiş River. The configuration of the flood hydrograph on the Timiş and Sebeş Rivers were considered as just mentioned, for the first one attached to *BC_S2D_11* line and the second to *BC_S2D_22* line. The program accomplished the distribution of the flow at the entrance on the edge condition lines. In the downstream edge, the hydrodynamic slope of *0.000375* was applied to the *BC_S2D_33* edge line. The actual numerical simulation of the flows transit was carried out for a given time period of significant hydrological phenomenon, starting on April 6^{th} at 11:40 p.m. and until April 7th at 9:40 a.m., 2000. The numerical analysis was performed for a time step Δt = *0.1* seconds, while the results storage was set for at a time interval of *10* minutes.

4. NUMERICAL SIMULATION AND OUTCOMES PRESENTATION

As running the numerical simulations, the steady and time-depending parameters were obtained, meaning levels, flows and velocities in all cross-sections of the *1D* numerical model and on each cell of the discrete 2D numerical models. Following the graphical post-processing operations, the numerical results were deposited in separate files. As considering the *2D* area, the outcome may be viewed for each cell or on user-defined paths, by the options in the *RAS Mapper*.

The following presentation of the *2D* model outcomes is only a reduced option with respect to the possible features of *HEC-RAS 6.2*. Thus, only a few significant options are selected for a comparative presentation between the 3 models made in *1D* and *2D*.

4.1 M1 – *1D* NUMERICAL MODEL

• The variation of the water surface on the *1D* model and a longitudinal comparison section on the slope route in *1D* (index *kz18*) and the same route in *2D* (index *kz7* – bridge connecting structure and index *kz8* – bridge with special elements in *3D*) – *Figure 7*. It can be noticed that the appreciation of the rowing area upstream of the bridge in the *M2* and *M3*, lead to a higher variation of the water level compared to the *M1*, respectively downstream of the bridge, the numerical values in the *M2* and *M3* are lower than in the one-dimensional M1 (the values associated with the *M2* and *M3* are closer to the real ones in all situations of current flow or at accidental flooding).

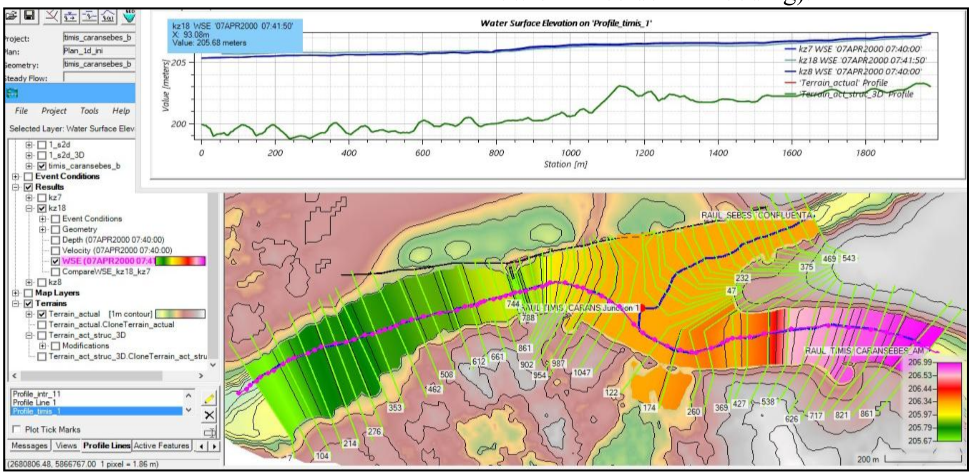

Figure 7. Water level distribution (in mSL) and a thalweg longitudinal profile for the three models *M1, M2* and *M3*

• The water velocity distribution on the *1D* model (*M1*, index *kz18*) and a cross-section through the axis of the connecting structure (*M2*), with the comparation of this parameter values for the 3 models: *M1* (index *kz18* in *1D)* and *M2* and *M3* (index *kz7,* respectively index *kz8*, in *2D*) are presented by *Figure 8*. Significant differences in values can be noticed when assessing the velocity in this cross view, especially in the area of the quadruple abutments and much different when assessing them on the *1D* model.

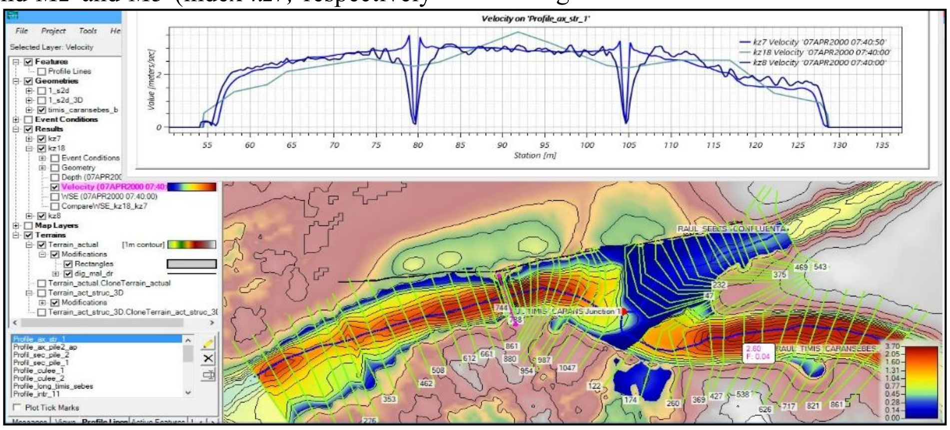

Figure 8. Water velocity distribution (in *m/s*) for the *1D* model and velocity comparation for the three models along the cross-view by the connection structure

4.2 M2 – *2D* NUMERICAL MODEL

• The water surface distribution of the on the *2D* model (index *kz7*, in *mSL*) and its development along a longitudinal profile by the water-course thalweg (the representation considers a limited magnification in the road bridge area in order to emphasize the variations on the 3 models) with respect to the *M1 and M3* (index *kz8*), the graphical representation corresponding to 07:40 a.m. on April 7th (*Figure 9*). There can be seen that the levels of the water surface in the longitudinal profile has similar values on the *M2* and *M3*, with higher values compared to the *M1* in the area upstream of the road bridge and respectively with lower values downstream of the bridge, which indicates an estimation closer to the real possible transit values in the situation of accidental flooding.

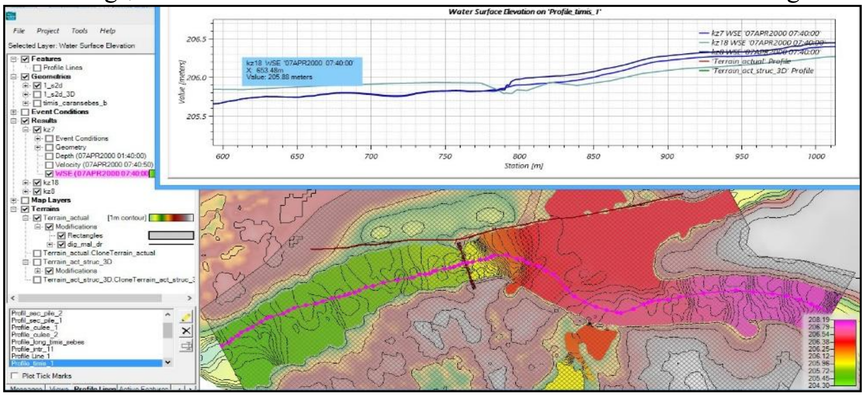

Figure 9. Water surface distribution for *M2* (in *mSL*) and its comparation with the M1 and M3 outcomes along a longitudinal profile by the water course thalweg

Particle trajectories plotting, superimposed to a detailed velocities distribution in the bridge area on the *2D* model (in *m/s, M2* – crossing road bridge connection structure), is given by *Figure 10*. It also presents a longitudinal profile by the intermediate abutment piers (intersecting the pillars from alignment 1 toward the left bank and 2 on the right bank). The levels graphic representations for the 3 models, *M1* (index *kz18*), *M2* (index *kz7*) and *M3* (index *kz8*), correspond to the time moment of 07:40 a.m. on April 7th, 2000. It is noted that the velocity appreciation in the area of the abutments in the *M1* is overestimated as compared to the outcomes in *M2* and *M3*. As for the *M3*, the velocity distribution seems as the closest to the real situation when transiting accidental flood flows.

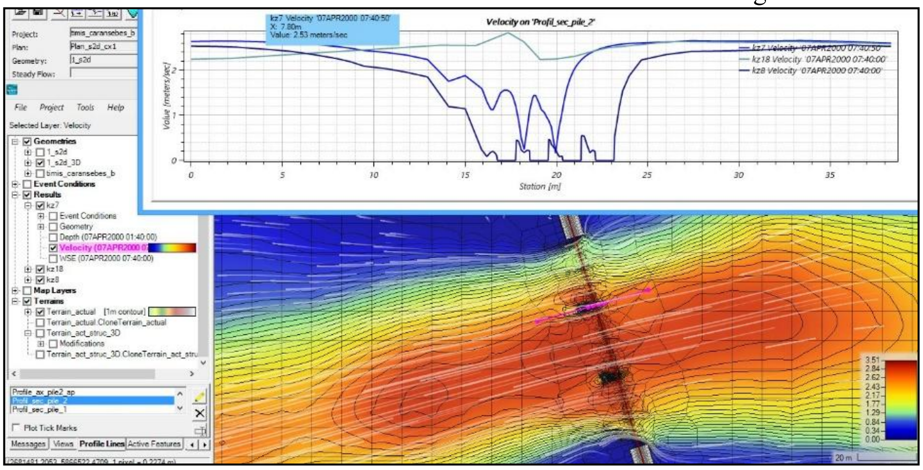

Figure 10. Velocity distribution for *M2* (in *m/s*) and its comparison with the *M1* and *M3* outcomes by a longitudinal profile in the area of the right-side abutment pier

4.3 M3 – *2D* STRUCTURE WITH SPECIAL ELEMENTS IN *3D*

• The water surface distribution (in *mSL*) in case of the *2D* model, with the crossing road bridge of special *3D* elements, in the structure associated area, and the velocity distribution (in *m/s*) in a cross-profile upstream of the piers (*Figure 11*). The graphic representations correspond also to the time moment of 07:40 a.m. on April 7th, 2000.

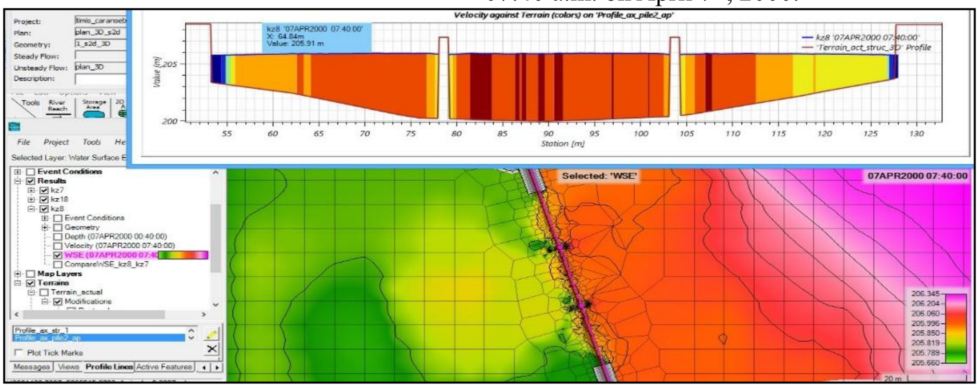

Figure 11. Detailed view of the water level distribution (in mSL) for *M3* with the velocity distribution in a cross-profile upstream of the bridge structure

The particle trajectories plotting overlaid to a detailed velocity distribution (in *m/s*) by the bridge area on the *2D* model (the *M3*, crossing road bridge with special *3D* elements), together with a cross-profile upstream of the abutment piers showing the level graphical representations for the 3 models (*M1*, index *kz18*, *M2*, index *kz7* and *M3*, index *kz8*). The representations correspond to 07:40 a.m. on April 7th (*Figure 12*). The considered cross-profile intersects the pillars in location 2 of the two alignments. The obtained level values on *M3* and *M2* are higher than the ones in *M1*, as being closer to the actual current flow or accidental floods situations.

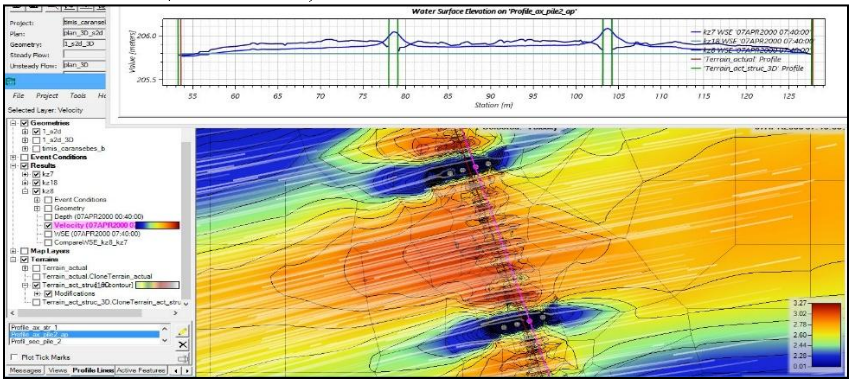

Figure 12. Particles trajectories overlaid to the limited view of water velocity distribution (in *m/s*) and a compared level distribution along a cross-profile upstream of the crossing structure, for the three models *M1*, *M2* and *M3*

Overlapped particle trajectories plotting over the velocity distribution (in *m/s*) for a limited area of the *2D* model (index *kz8*) and a longitudinal profile by the alignment *1* of the quadruple piles, for the 3 models, *M1* (index *kz18*), *M2* (index *kz7*) and *M3* (index *kz8*). The graphic representations correspond to the current time of 07:40 a.m. on April 7th, 2000 (*Figure 13*).

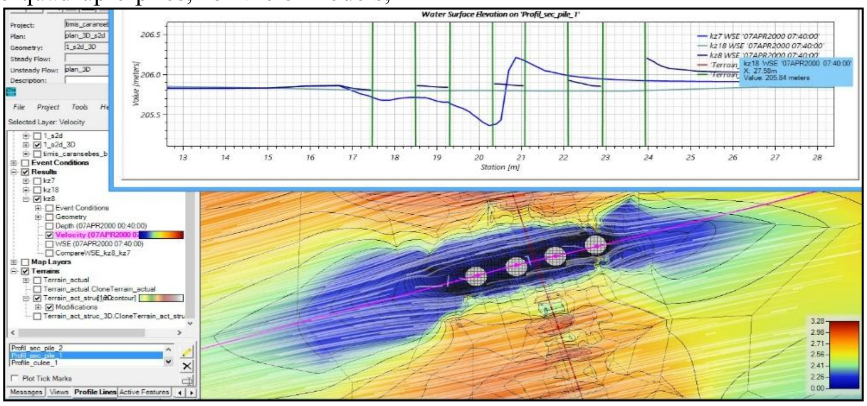

Figure 13. Particles trajectories overlaid to a detailed velocity distribution (in *m/s*) in the area of alignment 1, towards the left bank, and the level distribution along a longitudinal profile by the same alignment

An overlapping particle trajectories plotting over a limited visualization of velocity distribution (in *m/s*) for the *2D* model (*kz8 index*) and a longitudinal profile by the pier columns on alignment 2 for the 3 models, *M1* (*kz18 index*), *M2* (*kz7 index*) and *M3* (*kz8* index), corresponding also to the time moment of 07:40 a.m. on April 7th, (*Figure 14*).

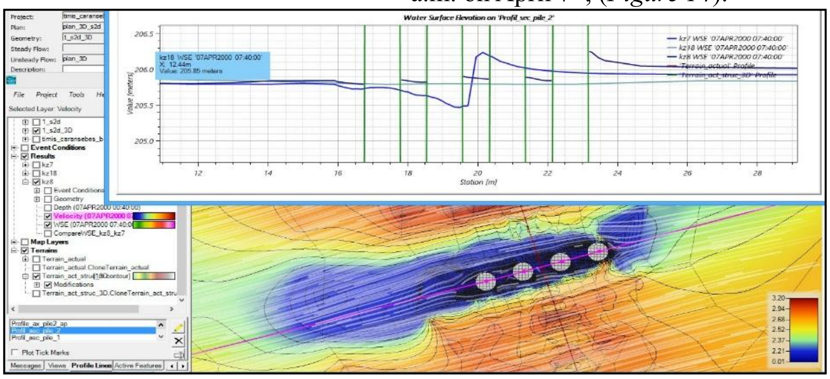

Figure 14. Particles trajectories overlaid to a detailed velocity distribution (in *m/s*) in the area of alignment 2, towards the right bank, and the level distribution along a longitudinal profile by the same alignment

5. COMPARATIVE STUDY. THE ***RASTER CALCULATOR*** FACILITY

- Comparative graphical representation for the water surface distribution between of first *2D* model (*M2,* index *kz7*) and *1D* model (*M1,* index *kz18*), with a limited visualization in the area of the quadruple piles, alignment 2 and, respectively, a profile by the piles in alignment 2, at 07:40 a.m. on April 7th, 2000 (*Figure 15*).

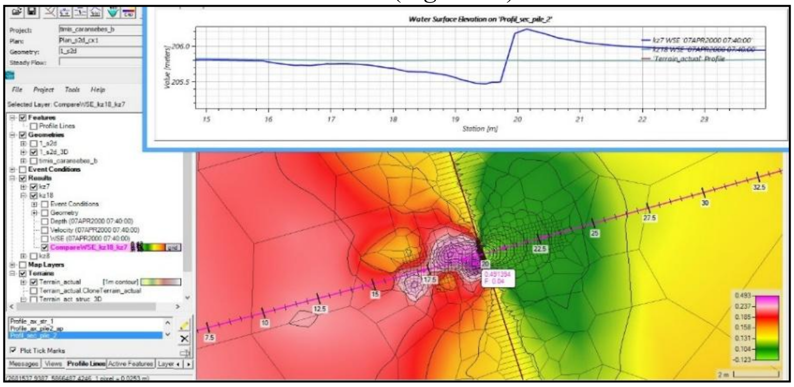

Figure 15. Water level distribution differences between *M1* and *M2*, also presented along a profile by alignment 2

- Comparative graphic representation on a limited visualization in the area of the quadruple piles in alignment *1*, showing the differences in water surface levels between *M1* (index *kz18*) and *M2* (index *kz7*), together with a longitudinal profile by the pillars in alignment *1*, at 07:40 a.m. on April 7th, 2000 (*Fig. 16*).

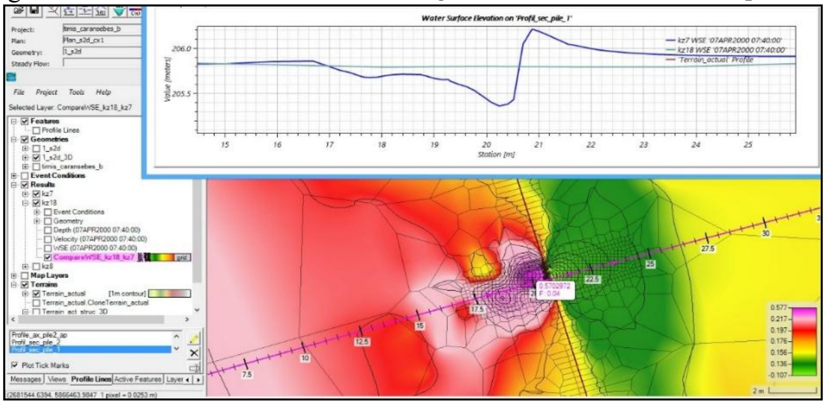

Figure 16. Water level distribution differences between *M1* and *M2*, also presented along a profile by alignment 1

- Comparative graphical representation on a limited visualization in the area of the quadruple piles alignment *1*, showing the differences in water surface levels between the two 2D models, *M3* (index *kz8*) and *M2* (index *kz7*), and a longitudinal profile by the pillars in alignment *1*, with the variation of the water levels on the 2 models *M2* and *M3*, at the time moment of 07:40 a.m. on April 7th, 2000 (*Figure 17*).

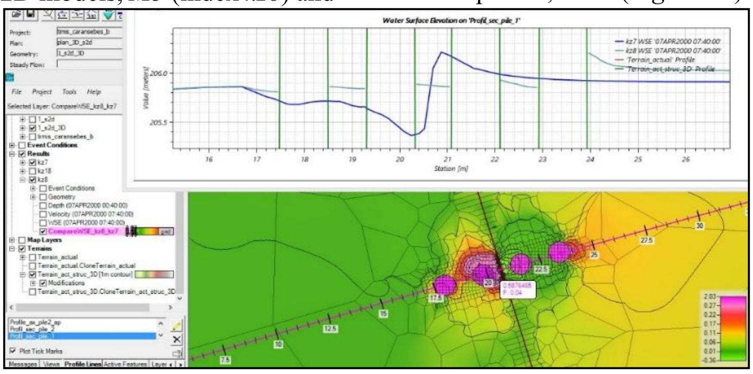

Figure 17. Water level distribution differences between *M3* and *M2*, also presented along a profile by alignment 1

- Comparative graphical representation on a limited visualization in the area of the quadruple piles of alignment *2*, showing differences in water surface levels between *M3* (index *kz8*) and *M2* (index *kz7*), together with a longitudinal water levels distribution by the pillars in alignment 2, at 07:40 a.m. on April 7th (*Figure 18*).

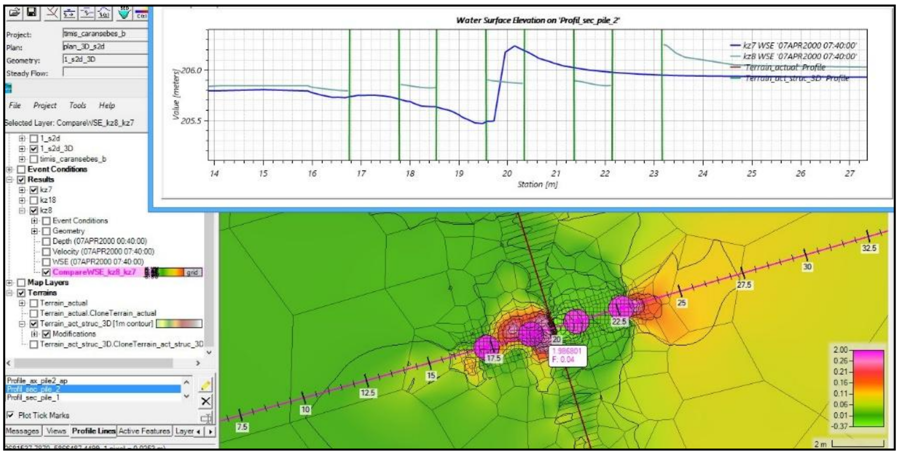

Figure 17. Water level distribution differences between *M3* and *M2*, with a longitudinal development along a profile by alignment 2

The differences in large values, of about *2.03* and *2.00*, represent the alteration in the geometric elevation in the upper area of the circular pillars in *2D* models (*M3*, index *kz8* and *M2*, index *kz7*). The other differences between the compared values, as presented in the values range (see legend), are within the limits of approx. *+0.27m* to *-0.36m* at alignment *1* (corresponding to the abutment pier towards the left bank) and within the limits of approx. *+0.26m* to *-0.37m* for alignment *2* (corresponding to the pier towards the right bank.

6. FINAL CONCLUSIONS

The presented paper uses the newer comparison feature in *HEC-RAS* by *RAS Mapper*, which allows mathematical and logical operations to be performed on gridded datasets, obtained by user-defined scripts. The comparison of the post-processed outcomes of two different models is used in a very similar way with a dynamic map, the associated layers can be animated in the two different *HEC-RAS* simulations, either in a *1D* (*M1*) *vs. 2D* (*M2*) representation or a *2D* (*M3*) *vs. 2D* (*M2*) representation.

The approximations on the resulting level distributions by the bridge area (piers area) for *M3* and *M2* are very close in representation (except for alignments 1 and 2) and much different (especially in the pier area) compared to the level variation for *M1*, either for a regular flow or for the exceptional flood wave.

It can be seen from the presented graphical visualizations that differences in level values are closer on the *M3* and *M2* models in intervals of about *+0.27m* ... *-0.36m* and *+0.26m* ...*- 0.37m*.

Therefore, it can be said that the representation of the levels and velocities in the area of the abutment piers on *M3* (where structure was modeled by special *3D* elements, while for *M2* was employed an approximation given by a connection structure associated with the bridge section) show as the closest to the real situation, both at the transit of current flows and the transit of an exceptional flood wave. And yet, in this case, only the possible interactive query tools are presented, and the animated toolbar was not used to evaluate, at different time steps, the comparative distribution of water levels when transiting an exceptional flood wave (in the paper, the comparisons made are presented only in the situation of the maximum levels reached).

REFERENCES

[1] *Gary W. Brunner*, HEC–RAS 4.1, River Analysis System Hydraulic Reference Manual, US Army Corps of Engineers, November 2002.

[2] HEC–GeoRAS GIS Tools for Support of HEC-RAS using ArcGIS User's Manual, Version 4.3.93, February 2011, US Army Corps of Engineers Institute for Water Resources Hydrologic Engineering Center.

[3] *Gerrit Kiers*, VIZITERV Consult Kft., Lifting Terrain in HEC-RAS 5.0 Copyright © The RAS Solution and Gerrit Kiers 2015.

[4] *Gary W. Brunner*, Combined 1D and 2D Modeling with HEC–RAS, October, vers.5 2016, US Army Corps of Engineers.

[5] HEC-RAS River Analysis System, Supplemental to HEC-RAS Version 5.0 User's Manual, Version 5.0.4 April 2018, US Army Corps of Engineers.

[6] HEC–RAS Mapper User's Manual vers. 6.0, December 2020, US Army Corps of Engineers.

[7] *Gary W. Brunner*, HEC–RAS 6.2 March 2021, US Army Corps of Engineers.

[8] *Mc Breach by Kleinschmidt*, Probabilistic Dam Breach Modeling, User's Manual, Version 5.07, June 2019, Porland, Oregon.

[9] *LAZĂR, Gh.I.,* Curs mapper ansamblu final ultrec, Note de curs, Timișoara, iulie, 2022.

[10] *Ghițescu, M.A., LAZĂR, Gh. I., Constantin, A.T., Nicoară, Ș.V.,* Alternative study on 1D and 2D numerical model in HEC□RAS 5.05, on the Timiș River, at the confluence with the Sebeș River, in the municipality of Caransebeș, upon the transit of an accidental flood wave

[11] *Nicoară, Ș.V., LAZĂR, Gh.I., Constantin, A.T.,* Comparative Study of a 1D and 2D Numerical Analysis Modelling a Water Flow at a River Confluence under Accidental High Waters, HIDRAULICA – Magazine of Hydraulics, Pneumatics, Tribology, Ecology, Sensorics, Mechatronics, ISSN 1453-730, nr. 4/2018.

[12] *Nicoară, Ș.V., LAZĂR, Gh.I., Constantin, A.T.*, 2D Numerical Model of a River Sector Flow in Case of Hypothetical Side Flooding Due to Embankment Failure, HIDRAULICA - Magazine of Hydraulics, Pneumatics, Tribology, Ecology, Sensorics, Mechatronics, ISSN 1453 – 7303, No.1/2019.

[13] *Nicoară, Ș.V., LAZĂR, Gh.I., Constantin, A.T.,* Computer Analysis of Water Flow Transition under Existing Conditions on a River Sector in the Range of a Bridge Structure, HIDRAULICA - Magazine of Hydraulics, Pneumatics, Tribology, Ecology, Sensorics, Mechatronics, ISSN 1453 – 7303, No.1/2019.

[14] *Ghițescu, M.A., LAZĂR, Gh. I., Constantin, A.T., Nicoară, Ș.V.*, Numerical Modeling of River Embankment Local Failure under Accidental High-Waters Conditions, HIDRAULICA - Magazine of Hydraulics, Pneumatics, Tribology, Ecology, Sensorics, Mechatronics, ISSN 1453 – 7303, No.3/2020.